

The progenitor of the FUor-type young eruptive star 2MASS J06593158–0405277¹

Á. Kóspál¹, P. Ábrahám¹, A. Moór¹, M. Haas², R. Chini^{2,3} and M. Hackstein²

ABSTRACT

Only a dozen confirmed FU Orionis-type young outbursting stars (FUors) are known today; this explains the interest in the recent FUor eruption of 2MASS J06593158–0405277. Its outburst and expected decline will be subject to numerous studies in the future. Almost equally important for the understanding of the eruption mechanism, however, is the physical characterization of the FUor’s precursor. Here we analyze unpublished archival data and summarize – and partly revise – all relevant photometry from optical to submillimeter wavelengths. Our analysis implies that the FUor is possibly associated with eight T Tauri star candidates and a strong Class 0 source. Adopting a distance of 450 pc for the FUor, we derive a quiescent bolometric luminosity and temperature of $L_{\text{bol}} = 4.8 L_{\odot}$ and $T_{\text{bol}} = 1190$ K, typical for young Class II sources. The central star has a temperature of $T_{\text{eff}} = 4000$ K, a mass of $0.75 M_{\odot}$, and an age of about 6×10^5 yr. The SED implies a circumstellar mass of $0.01 - 0.06 M_{\odot}$, and the system is surrounded by a faint infrared nebulosity. Our results provide an almost complete picture of a FUor progenitor, supporting the interpretation of future post-outburst studies.

Subject headings: stars: pre-main sequence — stars: individual (2MASS J06593158–0405277)

¹Konkoly Observatory, Research Centre for Astronomy and Earth Sciences, Hungarian Academy of Sciences, PO Box 67, H-1525 Budapest, Hungary

²Astronomisches Institut, Ruhr-Universität Bochum, Universitätsstraße 150, D-44801 Bochum, Germany

³Instituto de Astronomía, Universidad Católica del Norte, Antofagasta, Chile

¹Based on observations made with the Herschel Space Observatory. Herschel is an ESA space observatory with science instruments provided by European-led Principal Investigator consortia and with important participation from NASA.

1. Introduction

Nascent Sun-like stars are surrounded by circumstellar material, which builds up the growing protostar as matter is accreted through a circumstellar disk. The accretion rate varies in time: the protostar’s normal accretion at a low rate ($\sim 10^{-8} M_{\odot} \text{ yr}^{-1}$) is occasionally interspersed by brief episodes of highly enhanced accretion (Kenyon et al. 1990). FU Orionis-type variables (FUors) are the visible examples of episodic accretion. During their episodic “outbursts”, accretion rate from the circumstellar disk onto the star increases by several orders of magnitude, leading to a 5–6 mag optical brightening (Hartmann & Kenyon 1996; Audard et al. 2014). The first FUors which defined the class (“*classical FUors*”) are in outburst for decades (Herbig 1977). As a consequence, information on their progenitors is almost non-existing. The most common assumption is that they are Class II, or Class I/Class II transitional objects with massive disks and (in many cases) extended envelopes. Recent results, however, demonstrate that deeply embedded Class I objects (e.g., V1647 Ori, Ábrahám et al. 2004b; OO Ser, Kóspál et al. 2007) and Class II objects with very small disk masses and no envelopes (e.g., HBC 722, Miller et al. 2011) could also show FUor-like eruptions. Another class of young eruptive stars, called EXors after the prototype EX Lup, exhibit typically smaller, shorter, repetitive outbursts (Herbig 1977, 2008).

On November 30, 2014, Maehara et al. (2014) reported the discovery of a new outbursting star, 2MASS J06593158–0405277. Optical spectra of the object obtained by Maehara et al. (2014) and by Hillenbrand (2014), and infrared spectra published by Reipurth & Connelley (2015) and by Pyo et al. (2015) are very similar to those of the classical FUors. Our group has been monitoring the area around this source with a robotic telescope at Bochum observatory near Cerro Armazones since 2010. The optical light curves show that the object started a slow rising at the end of 2013, and quickly brightened by about 3 mag both in r and i compared to the quiescent level, reaching peak brightness at the end of October 2014 (Hackstein et al. 2014).

Thanks to the object’s proximity to the Galactic plane, its position was covered with a number of all-sky or Galactic plane surveys, providing information on the system in its quiescent phase. Thus, 2MASS J06593158–40405277 offers a unique opportunity to study the progenitor of a classical FUor. Here, we collect and analyze archival optical, infrared and submillimeter observations of the new outbursting star (hereafter, “the FUor”), and discuss the structure of its circumstellar and interstellar environment. Our study will serve as a basis for future work on the object in outburst, including possible changes in the circumstellar matter induced by the eruption.

2. Optical/infrared/submillimeter data

Optical data. The FUor is visible in the digitized Palomar Observatory Sky Survey images. However, its magnitudes in the USNO-B1.0 catalog (Monet et al. 2003) probably suffer from source confusion due to a close-by star $5''.7$ to the north (2MASS J06593168–0405224, hereafter, “N component”). We repeated the photometry using a small, $3''$ radius aperture. For calibration, we selected all those nearby stars within $10'$ whose instrumental magnitudes differ less than ± 0.1 mag from that of our target. Plotting their USNO-B1.0 magnitudes as a function of the instrumental magnitude, the distribution of data points could be fitted with a linear relationship. We used this linear fit to determine the magnitude of the FUor (Table 1). Due to its faintness and proximity to the FUor, no reasonable photometry could be obtained for the N component.

Near-infrared data. JHK_S magnitudes for the FUor in quiescent phase are available in the 2MASS catalog (Cutri et al. 2003). The source was also covered in the DENIS (Epchtein 1998) and UKIDSS (Lawrence et al. 2007) near-infrared sky surveys. For the sake of homogeneous calibration, we performed aperture photometry on the DENIS and UKIDSS images, using a $3''$ radius aperture, and adopting nearby sources from the 2MASS catalog as photometric standards in the JHK_S bands. In the DENIS I band, we used the magnitudes of the comparison stars from the DENIS catalog. The resulting near-infrared photometry is listed in Table 1. Additionally, we obtained photometry for a number of fainter sources visible in the UKIDSS images in the vicinity of the FUor, whose colors will be analyzed in Sec. 3.1. These values are listed in Table 2.

Mid- and far-infrared data. The area around the FUor was observed by the Infrared Array Camera (IRAC, Fazio et al. 2004) on-board the Spitzer Space Telescope (Werner et al. 2004) at 3.6 and $4.5 \mu\text{m}$. We took photometry for the FUor from the GLIMPSE360 Catalog (Churchwell et al. 2009) and obtained psf-photometry for the N component using the idl-based tool STARFINDER (Diolaiti et al. 2000). The FUor was also covered by the Mid-course Space Experiment (MSX, Egan et al. 2003), resulting a $8.28 \mu\text{m}$ flux in the MSX6C Point Source Catalog. The Wide-field Infrared Survey Explorer (WISE, Wright et al. 2010) observed our source in all four bands on April 1–2, 2010 in the cryogenic mission, and in the two shorter wavelength bands on October 10–11, 2010, as part of the post-cryo mission. At 3.35 and $4.60 \mu\text{m}$ we used data from the ALLWISE Multiepoch Photometry Table and averaged the April and October data points separately. At 11.56 and $22.09 \mu\text{m}$, we used the ALLWISE Source Catalog, that combines all data from the WISE mission. The FUor was also covered by the AKARI mission (Murakami et al. 2007). It is present in the AKARI/IRC

All-Sky Survey Point Source Catalogue, with photometry at 9 and 18 μm .

Far-infrared and submillimeter data. The area around the FUor was observed with the Herschel Space Observatory (Pilbratt et al. 2010) in the PACS/SPIRE parallel mode (Poglitsch et al. 2010; Griffin et al. 2010). We processed the PACS 70 and 160 μm data with the Herschel Interactive Processing Environment v.13 (HIPE, Ott 2010) using the standard script optimized for mapping observations. We used the recently developed gyro correction to reduce the pointing jitter. The final 70 and 160 μm maps were made with the PHOTPROJECT task. At 70 μm , two point sources are detectable: one corresponding to the FUor, while the other source is located 5".9 to the southeast (hereafter, "SE component"). We used 3" radius apertures to measure the flux ratio of these two targets, then measured the total flux in a large 22" radius aperture, and divided it between the two targets according to their flux ratio. At 160 μm , the two sources are not well resolved any more, but the centroid of the image is within 1".2 of the 70 μm position of the SE component, indicating that at this wavelength, the SE source dominates the emission. At this wavelength, photometry was obtained in a 22" radius aperture. The fluxes, whose uncertainties include the 7% overall calibration uncertainty of the PACS photometer, are presented in Table 1. To derive photometry in the SPIRE 250, 350, and 500 μm bands, we used the TIMELINE FITTER task of HIPE (Bendo et al. 2013) to fit circular Gaussians to the baseline-subtracted timeline data. Here again, the centroid of the source corresponds to the SE component, and not to the FUor. The resulting fluxes, whose uncertainties include the 5.5% overall calibration uncertainty of the SPIRE photometer, are presented in Table 1. The AKARI/FIS All-Sky Survey Point Source Catalogue contains a source which is closer to the SE component than to the FUor. While the photometry at 65 μm probably suffers from confusion of these two targets, the fluxes at longer wavelengths can be safely attributed to the SE component.

3. Results and analysis

3.1. The broader environment

Fig. 1 displays the region around the FUor at different wavelengths revealing a complex environment. The FUor itself is well visible between the optical and 70 μm . The N component is located at a separation of 5".7, PA of 15°, clearly discernible until 4.5 μm , and possibly present even in the WISE bands. The SE component is located at a distance of 5".9, PA of 157°. This source is first visible at 70 μm , and we could not unambiguously link it to any point sources at shorter wavelengths. At 70 μm it is already brighter than the FUor and clearly dominates the emission at longer wavelengths.

The deep UKIDSS images reveal a faint nebulosity around the FUor, especially apparent to the south but visible to the west as well (Fig. 1, right). Its characteristic size is $\approx 15''$. This extended emission is also discernible in the IRAC images. The nebulosity, especially its southern part, is much redder than the FUor itself. If the origin of the nebulosity is light from the FUor scattered by the circumstellar matter, then the nebulosity should be bluer than the light source, unless it is reddened by some dust along the line-of-sight. We speculate that the extinction needed for this may be provided by the massive envelope of the SE component.

In order to find out whether the FUor is an isolated young star or there are other pre-main sequence objects in its vicinity, we obtained photometry on the UKIDSS images for several point sources within $1'$ of the FUor. By plotting the objects on a $J - H$ vs. $H - K_S$ color-color diagram (Fig. 2, left), we found that most of them are on the main sequence, or they are reddened main sequence stars with extinction up to $A_V = 6$ mag. In addition to the FUor, we found eight stars around the T Tauri locus (Meyer et al. 1997), one being the N component, while the other seven are marked in Table 2. This indicates that they are young stellar object candidates, thus the FUor is probably not isolated.

3.2. Variability in quiescence

In Table 1 we collected all available pre-outburst photometry for the FUor. In the $0.4\text{--}5\ \mu\text{m}$ range, multi-epoch data is available, making it possible to search for variability in the quiescent phase. Significant flux changes up to 0.7 mag are revealed when comparing the two different red Palomar points, and also the infrared Palomar and DENIS I -band points. In the J , H , and K_S bands and in the $3\text{--}5\ \mu\text{m}$ range, the object was constant within 0.15 mag. This indicates that the object has a well-defined quiescent state, with accretion rate changes probably much smaller than what caused the recent outburst.

3.3. Colors and spectral energy distribution

Based on the photometry in Table 1, we plotted the pre-outburst spectral energy distribution (SED) of the FUor in Figure 3 with dots, the N component with squares, and the SE component with asterisks. We only used points which can be unambiguously attributed to either of these three sources. Thus, the AKARI/FIS point at $65\ \mu\text{m}$, where the FUor and the SE source are probably blended together, is omitted.

The SED of the FUor indicates significant infrared emission from the circumstellar

matter. On the $J - H$ vs. $H - K_S$ color-color diagram (Fig. 2, left), the object falls onto the T Tauri locus (Meyer et al. 1997), suggesting that it is a regular T Tauri star with negligible reddening ($A_V < 0.5$ mag). Indeed, its optical–near-infrared SED (up to the H band) can be reasonably well fitted using a Kurucz model of a late K-type or early M-type photosphere with effective temperatures between 3750 K and 4250 K (Fig. 3). Excess emission compared to the stellar photosphere appears first in the K_S band. Until about $12 \mu\text{m}$, the SED decreases like $\nu F_\nu \sim \lambda^{-0.5}$, typical for moderately flared disks (Kenyon & Hartmann 1987). After about $12 \mu\text{m}$, the SED starts rising again, suggesting the presence of an outer envelope.

The N component has a SED shape similar to the FUor, indicating that it is probably a T Tauri star as well, but with lower temperature and mass. Indeed, it falls onto the T Tauri locus in the near-infrared color-color diagram (see also Sec. 3.1 and Fig. 2, left). The SE component is probably a deeply embedded Class 0 object, invisible in the optical, and peaking at around $160 \mu\text{m}$. Its submillimeter spectral slope is $\nu F_\nu \sim \lambda^{-2.5}$.

3.4. Distance

The FUor is situated in the Galactic plane ($l = 217.5$, $b = -0.1$). The Herschel images of this area suggest that it sits on top of a long, elongated filament corresponding to the LDN 1650 molecular cloud (also known as S 287). CO observations by, e.g., Kim et al. (2004) suggest a velocity of $v_{\text{LSR}} = 26\text{--}28 \text{ km s}^{-1}$ for the molecular gas, which gives a kinematic distance of 2.3 kpc. However, supposing that the FUor is a low-mass pre-main sequence star, as suggested by its optical–near-infrared SED (Sect. 3.3), its apparent brightness contradicts this relatively large distance.

The pre-main sequence evolutionary tracks of Siess et al. (2000) predict that the absolute J magnitude of a star in the 3750–4250 K temperature range should be between 2 and 4 mag for ages between 5×10^5 and 2×10^6 yr (Fig. 2, right). The apparent $J = 11$ mag would then correspond to a distance range of 250–630 pc for the FUor. If the object is located at 2.3 kpc, its absolute J magnitude would be -0.8 mag, typical for much higher temperature young objects. The observed SED, however, peaks at near-infrared wavelengths, and could be consistent with a higher temperature photosphere only if significantly reddened. For instance, a $T_{\text{eff}} = 6000$ K photosphere with $A_V = 2.3$ mag reddening would adequately fit the SED until the J band. Thus, due to the well-known degeneracy between the stellar temperature and the interstellar extinction, the central star can either be an unreddened low-mass M-type young star at a distance of about 450 pc (a representative value between 250 and 630 pc), or a moderately reddened intermediate-mass F-type young star at a distance of 2.3 kpc.

Without a pre-outburst optical spectrum that could be used for stellar classification, it is very difficult to decide whether the FUor is an unreddened M-star close-by, or a reddened F-star far away. There is, however, extra information that we can use to decide. We scaled a blackbody function to the $70\ \mu\text{m}$ flux of the FUor, extrapolated to $850\ \mu\text{m}$, and used this flux prediction to estimate the total mass of the circumstellar matter. We adopted a gas-to-dust mass ratio of 100. Assuming 55 K or 100 K for the dust temperature, we obtained $0.06 M_{\odot}$ or $0.01 M_{\odot}$, respectively, for a distance of 450 pc, and $1.6 M_{\odot}$ or $0.28 M_{\odot}$ for a distance of 2.3 kpc. A similar estimate can be done for the SE component using the $500\ \mu\text{m}$ SPIRE flux. Here we used 50 K or 20 K, and obtained $0.31 M_{\odot}$ or $1.3 M_{\odot}$, respectively, for 450 pc, and $8.2 M_{\odot}$ or $34 M_{\odot}$ for 2.3 kpc. In the Galactic plane there is no guarantee that the FUor and the SE source is at the same distance. However, the fact that there is at least 2 (or possible a few more) T Tauri stars and an embedded submillimeter source all within $1'$ strongly suggests that they are associated to each other. In this case, the larger distance would give an unrealistically large total mass for the SE component. Therefore, we suggest that the young stellar objects in this area, including new outbursting star, are not associated with LDN 1650, but located much closer to us, probably around $d = 450\ \text{pc}$. We will use this distance value in our subsequent discussion.

4. Discussion

In the following, we discuss the physical nature of the FUor in quiescence. The central star is a low-mass young star, with effective temperature of about $T_{\text{eff}} = 4000\ \text{K} \pm 250\ \text{K}$ (Sec. 3.3). The Siess models in Fig. 2 predict a stellar mass of $M_* = 0.75 M_{\odot} \pm 0.25 M_{\odot}$. By integrating the SED in Fig. 3, we obtained a stellar luminosity of $L_* = 1.2 L_{\odot}$ and a total bolometric luminosity is $L_{\text{bol}} = 4.8 L_{\odot}$. Following Chen et al. (1995), we determined the bolometric temperature of the object, which is a distance-independent quantity. The resulting $T_{\text{bol}} = 1190\ \text{K}$ indicates that the object is Class II (their Fig. 6), and its age is approximately $6 \times 10^5\ \text{yr}$ (their Fig. 4).

The circumstellar structure of the FUor resembles the canonical picture of classical FUors (Hartmann & Kenyon 1996), where a young T Tauri star is surrounded by a moderately flared circumstellar disk and an envelope. In our case, the total circumstellar mass is on the order of $0.01\text{--}0.06 M_{\odot}$, falling into the range of typical T Tauri disks (Beckwith et al. 1990), and is somewhat lower than envelope masses measured by Sandell & Weintraub (2001) and by Kóspál (2011) for FUors. The SED shows a conspicuous break at $12\ \mu\text{m}$, which may indicate an inner hole in the envelope. Additionally, the envelope must have a cavity as well, through which we have an unobscured view of the star and the inner disk.

The comparison of the SED with other classical FUors is not straightforward, because for them, only outburst SEDs are known (Ábrahám et al. 2004a). For this reason, we compare the SED in Fig. 3 to the quiescent SED of the young eruptive star V1647 Ori dereddened by $A_V=13$ mag (Fig. 3 in Ábrahám et al. 2004b). The two SEDs exhibit similar shapes, and it is remarkable that even their absolute flux levels agree within a factor of 3 in the whole 1–70 μm range, strengthening our distance estimate for the FUor. From an evolutionary point of view, Quanz et al. (2007) and Green et al. (2006) proposed that FUors are young stars in transition from the Class I to Class II. The transition process is associated with the gradual dispersion of the envelope due to the repetitive outbursts. In this picture, our results on the progenitor of the classical FUor candidate 2MASS J06593158–0405277 indicate that it is an evolved FUor, approaching the evolutionary phase of a disk-only T Tauri star.

This work was supported by the Momentum grant of the MTA CSFK Lendület Disk Research Group, and the Hungarian Research Fund OTKA grant K101393. A. M. acknowledges support from the Bolyai Research Fellowship of the Hungarian Academy of Sciences.

Facilities: Spitzer, Herschel, WISE, AKARI.

REFERENCES

- Ábrahám, P., Kóspál, Á., Csizmadia, S., et al. 2004a, *A&A*, 428, 89
- . 2004b, *A&A*, 419, L39
- Audard, M., Ábrahám, P., Dunham, M. M., et al. 2014, *ArXiv e-prints*
- Beckwith, S. V. W., Sargent, A. I., Chini, R. S., & Guesten, R. 1990, *AJ*, 99, 924
- Bendo, G. J., Griffin, M. J., Bock, J. J., et al. 2013, *MNRAS*, 433, 3062
- Cardelli, J. A., Clayton, G. C., & Mathis, J. S. 1989, *ApJ*, 345, 245
- Chen, H., Myers, P. C., Ladd, E. F., & Wood, D. O. S. 1995, *ApJ*, 445, 377
- Churchwell, E., Babler, B. L., Meade, M. R., et al. 2009, *PASP*, 121, 213
- Cutri, R. M., & et al. 2014, *VizieR Online Data Catalog*, 2328, 0
- Cutri, R. M., Skrutskie, M. F., van Dyk, S., et al. 2003, *VizieR Online Data Catalog*, 2246,

- Diolaiti, E., Bendinelli, O., Bonaccini, D., et al. 2000, *The Messenger*, 100, 23
- Egan, M. P., Price, S. D., Kraemer, K. E., et al. 2003, *VizieR Online Data Catalog*, 5114, 0
- Epchtein, N. 1998, in *IAU Symposium, Vol. 179, New Horizons from Multi-Wavelength Sky Surveys*, ed. B. J. McLean, D. A. Golombek, J. J. E. Hayes, & H. E. Payne, 106
- Fazio, G. G., Hora, J. L., Allen, L. E., et al. 2004, *ApJS*, 154, 10
- Green, J. D., Hartmann, L., Calvet, N., et al. 2006, *ApJ*, 648, 1099
- Griffin, M. J., Abergel, A., Abreu, A., et al. 2010, *A&A*, 518, L3
- Hackstein, M., Chini, R., Haas, M., Abraham, P., & Kospal, A. 2014, *The Astronomer's Telegram*, 6838, 1
- Hartmann, L., & Kenyon, S. J. 1996, *ARA&A*, 34, 207
- Herbig, G. H. 1977, *ApJ*, 217, 693
- . 2008, *AJ*, 135, 637
- Hillenbrand, L. 2014, *The Astronomer's Telegram*, 6797, 1
- Ishihara, D., Onaka, T., Kataza, H., et al. 2010, *A&A*, 514, A1
- Kenyon, S. J., & Hartmann, L. 1987, *ApJ*, 323, 714
- Kenyon, S. J., Hartmann, L. W., Strom, K. M., & Strom, S. E. 1990, *AJ*, 99, 869
- Kim, B. G., Kawamura, A., Yonekura, Y., & Fukui, Y. 2004, *PASJ*, 56, 313
- Koornneef, J. 1983, *A&A*, 128, 84
- Kóspál, Á. 2011, *A&A*, 535, A125
- Kóspál, Á., Ábrahám, P., Prusti, T., et al. 2007, *A&A*, 470, 211
- Lawrence, A., Warren, S. J., Almaini, O., et al. 2007, *MNRAS*, 379, 1599
- Maehara, H., Kojima, T., & Fujii, M. 2014, *The Astronomer's Telegram*, 6770, 1
- Meyer, M. R., Calvet, N., & Hillenbrand, L. A. 1997, *AJ*, 114, 288
- Miller, A. A., Hillenbrand, L. A., Covey, K. R., et al. 2011, *ApJ*, 730, 80
- Monet, D. G., Levine, S. E., Canzian, B., et al. 2003, *AJ*, 125, 984

- Murakami, H., Baba, H., Barthel, P., et al. 2007, PASJ, 59, 369
- Ott, S. 2010, in Astronomical Society of the Pacific Conference Series, Vol. 434, Astronomical Data Analysis Software and Systems XIX, ed. Y. Mizumoto, K.-I. Morita, & M. Ohishi, 139
- Pilbratt, G. L., Riedinger, J. R., Passvogel, T., et al. 2010, A&A, 518, L1
- Poglitsch, A., Waelkens, C., Geis, N., et al. 2010, A&A, 518, L2
- Pyo, T.-S., Oh, H., Yuk, I.-S., Kim, H., & Davis, C. J. 2015, The Astronomer’s Telegram, 6901, 1
- Quanz, S. P., Henning, T., Bouwman, J., et al. 2007, ApJ, 668, 359
- Reipurth, B., & Connelley, M. S. 2015, The Astronomer’s Telegram, 6862, 1
- Sandell, G., & Weintraub, D. A. 2001, ApJS, 134, 115
- Siess, L., Dufour, E., & Forestini, M. 2000, A&A, 358, 593
- Werner, M. W., Roellig, T. L., Low, F. J., et al. 2004, ApJS, 154, 1
- Wright, E. L., Eisenhardt, P. R. M., Mainzer, A. K., et al. 2010, AJ, 140, 1868
- Yamamura, I., Makiuti, S., Ikeda, N., et al. 2010, VizieR Online Data Catalog, 2298, 0

Table 1. Photometry of the FUor 2MASS J06593158–0405277 and nearby objects

Instrument/Catalog	Filter/Wavelength (μm)	Date	Magnitude/Flux FUor	Magnitude/Flux N component	Magnitude/Flux SE component	Reference
Palomar	B1 / 0.425	1953-01-17	15.20 ± 0.1 mag	1
Palomar	R1 / 0.645	1953-01-17	12.47 ± 0.1 mag	1
Palomar	B2 / 0.463	1983-01-17	15.18 ± 0.1 mag	1
Palomar	R2 / 0.660	1989-03-05	12.97 ± 0.1 mag	1
Palomar	I / 0.808	1982-01-22	11.82 ± 0.1 mag	1
2MASS	J / 1.235	1998-11-02	11.049 ± 0.030 mag	13.500 ± 0.054 mag	...	2
2MASS	H / 1.662	1998-11-02	10.122 ± 0.036 mag	12.445 ± 0.068 mag	...	2
2MASS	Ks / 2.159	1998-11-02	9.452 ± 0.027 mag	11.611 ± 0.029 mag	...	2
DENIS	I / 0.791	1997-01-11	12.525 ± 0.020 mag	14.842 ± 0.027 mag	...	1
DENIS	J / 1.228	1997-01-11	11.003 ± 0.060 mag	13.266 ± 0.075 mag	...	1
DENIS	Ks / 2.145	1997-01-11	9.329 ± 0.050 mag	11.488 ± 0.088 mag	...	1
UKIDSS	J / 1.235	2010-01-01	11.030 ± 0.022 mag	13.688 ± 0.031 mag	...	1
UKIDSS	H / 1.662	2010-01-01	10.112 ± 0.017 mag	12.550 ± 0.035 mag	...	1
UKIDSS	Ks / 2.159	2010-01-01	9.460 ± 0.043 mag	11.628 ± 0.033 mag	...	1
UKIDSS	Ks / 2.159	2006-11-30	9.382 ± 0.058 mag	11.690 ± 0.037 mag	...	1
Spitzer/IRAC	3.6	2011-06-05	8.121 ± 0.045 mag	10.570 ± 0.070 mag	...	3
Spitzer/IRAC	4.5	2011-06-05	7.448 ± 0.026 mag	9.925 ± 0.030 mag	...	3
MSX	A / 8.28	1996-05 – 1997-01	5.987 ± 0.059 mag	4
WISE	W1 / 3.35	2010-04-01/02	8.063 ± 0.023 mag	5
WISE	W1 / 3.35	2010-10-10/11	8.106 ± 0.023 mag	5
WISE	W2 / 4.60	2010-04-01/02	7.186 ± 0.022 mag	5
WISE	W2 / 4.60	2010-10-10/11	7.232 ± 0.020 mag	5
WISE	W3 / 11.56	2010-04-01/02	5.240 ± 0.016 mag	6
WISE	W4 / 22.09	2010-04-01/02	2.219 ± 0.018 mag	6
AKARI/IRC	9	2006-05 – 2006-11	5.690 ± 0.022 mag	7
AKARI/IRC	18	2006-05 – 2006-11	3.146 ± 0.049 mag	7
AKARI/FIS	65	2006-05 – 2006-11	6.723 ± 1.826 Jy	8
AKARI/FIS	90	2006-05 – 2006-11	9.396 ± 0.734 Jy	8
AKARI/FIS	140	2006-05 – 2006-11	23.751 ± 3.448 Jy	8
AKARI/FIS	160	2006-05 – 2006-11	21.203 ± 2.879 Jy	8
Herschel/PACS	70	2011-05-08	3.54 ± 0.62 Jy	...	4.90 ± 0.62 Jy	1
Herschel/PACS	160	2011-05-08	20.9 ± 1.89 Jy	1
Herschel/SPIRE	250	2011-05-08	8.83 ± 0.50 Jy	1
Herschel/SPIRE	350	2011-05-08	6.24 ± 0.35 Jy	1

Table 1—Continued

Instrument/Catalog	Filter/Wavelength (μm)	Date	Magnitude/Flux FUor	Magnitude/Flux N component	Magnitude/Flux SE component	Reference
Herschel/SPIRE	500	2011-05-08	3.83 ± 0.22 Jy	1

Note. — References: 1 – this work; 2 – 2MASS All-Sky Catalog of Point Sources (Cutri et al. 2003); 3 – GLIMPSE360 Catalog (Churchwell et al. 2009); 4 – MSX6C Infrared Point Source Catalog (Egan et al. 2003); 5 – ALLWISE Multiepoch Photometry Table (Cutri & et al. 2014); 6 – ALLWISE Source Catalog (Cutri & et al. 2014); 7 – AKARI/IRC All-Sky Survey Point Source Catalogue (Ishihara et al. 2010); 8 – AKARI/FIS All-Sky Survey Point Source Catalogue (Yamamura et al. 2010)

Table 2. UKIDSS photometry for sources within 1' of the FUor
2MASS J06593158–0405277

	RA _{J2000}	DEC _{J2000}	<i>J</i> mag	<i>H</i> mag	<i>K_S</i> mag
	06:59:28.47	−04:05:51.84	13.25 ± 0.03	12.96 ± 0.04	12.90 ± 0.03
	06:59:28.63	−04:05:46.55	12.64 ± 0.03	12.41 ± 0.04	12.35 ± 0.03
T	06:59:28.67	−04:06:04.54	16.10 ± 0.03	15.00 ± 0.04	14.30 ± 0.03
T	06:59:28.90	−04:04:50.50	18.44 ± 0.06	17.17 ± 0.04	16.34 ± 0.03
	06:59:28.95	−04:05:01.30	17.23 ± 0.03	16.57 ± 0.04	16.14 ± 0.03
T	06:59:29.10	−04:05:11.11	17.89 ± 0.03	16.65 ± 0.04	15.66 ± 0.03
	06:59:29.58	−04:05:34.60	16.83 ± 0.03	16.19 ± 0.04	15.93 ± 0.03
	06:59:30.00	−04:05:05.06	17.83 ± 0.06	16.60 ± 0.04	15.89 ± 0.03
	06:59:30.11	−04:06:14.84	18.28 ± 0.05	17.61 ± 0.05	17.20 ± 0.08
	06:59:30.31	−04:04:56.04	15.04 ± 0.03	14.84 ± 0.04	14.86 ± 0.03
	06:59:30.36	−04:04:57.08	14.82 ± 0.03	14.43 ± 0.04	14.33 ± 0.03
	06:59:30.39	−04:06:01.22	12.22 ± 0.03	12.06 ± 0.04	12.02 ± 0.03
	06:59:30.49	−04:05:41.42	12.87 ± 0.03	12.66 ± 0.04	12.61 ± 0.03
	06:59:30.51	−04:06:09.42	16.43 ± 0.03	15.49 ± 0.04	14.95 ± 0.03
	06:59:30.87	−04:05:57.09	13.13 ± 0.03	12.86 ± 0.04	12.79 ± 0.03
	06:59:30.94	−04:06:22.94	17.25 ± 0.03	16.48 ± 0.04	16.13 ± 0.03
	06:59:31.01	−04:05:06.78	16.39 ± 0.03	15.73 ± 0.04	15.55 ± 0.03
	06:59:31.40	−04:06:20.01	17.65 ± 0.03	16.68 ± 0.04	16.26 ± 0.03
	06:59:31.87	−04:05:42.41	16.28 ± 0.03	15.09 ± 0.04	14.42 ± 0.03
T	06:59:31.89	−04:05:24.93	16.53 ± 0.03	15.71 ± 0.04	14.97 ± 0.03
	06:59:32.00	−04:05:46.88	16.31 ± 0.03	15.36 ± 0.04	15.02 ± 0.03
	06:59:32.36	−04:06:11.75	13.75 ± 0.03	13.51 ± 0.04	13.45 ± 0.03
T	06:59:32.45	−04:05:37.84	17.21 ± 0.03	16.38 ± 0.04	15.83 ± 0.04
T	06:59:32.47	−04:04:49.12	18.89 ± 0.08	17.89 ± 0.06	17.25 ± 0.08
T	06:59:32.71	−04:05:11.40	18.32 ± 0.05	17.72 ± 0.05	17.06 ± 0.07
	06:59:32.85	−04:05:12.88	18.49 ± 0.06	17.90 ± 0.06	17.81 ± 0.14
	06:59:32.97	−04:04:59.10	19.12 ± 0.11	17.81 ± 0.07	17.09 ± 0.08
	06:59:33.08	−04:04:49.46	15.57 ± 0.03	14.55 ± 0.04	13.94 ± 0.03
	06:59:33.26	−04:05:06.37	17.71 ± 0.03	16.53 ± 0.04	15.84 ± 0.03
	06:59:33.61	−04:06:05.09	18.90 ± 0.08	17.93 ± 0.06	17.53 ± 0.11
	06:59:33.74	−04:05:32.00	18.06 ± 0.04	16.80 ± 0.04	16.14 ± 0.03
	06:59:34.15	−04:05:21.60	17.89 ± 0.03	17.19 ± 0.04	16.94 ± 0.06
	06:59:34.75	−04:06:12.32	17.47 ± 0.03	16.67 ± 0.04	16.24 ± 0.04
	06:59:34.76	−04:04:56.32	17.01 ± 0.03	16.23 ± 0.04	15.97 ± 0.03

Note. — T marks T Tauri star candidates.

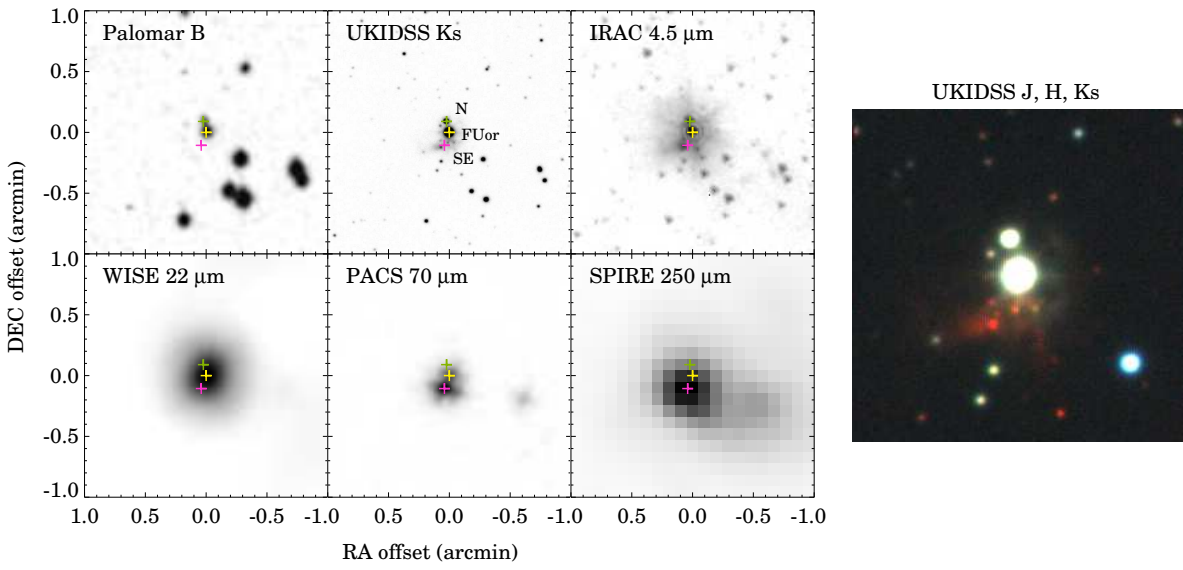


Fig. 1.— 2MASS J06593158–0405277 and its surroundings at different wavelengths. Yellow plus sign marks the optical stellar position of the FUor, magenta plus sign marks the SE component, and green plus marks the N component. The zoom-in on the right shows a color-composite image of an area of $50'' \times 50''$ centered on the FUor using J as blue, H as green, and K_S as red.

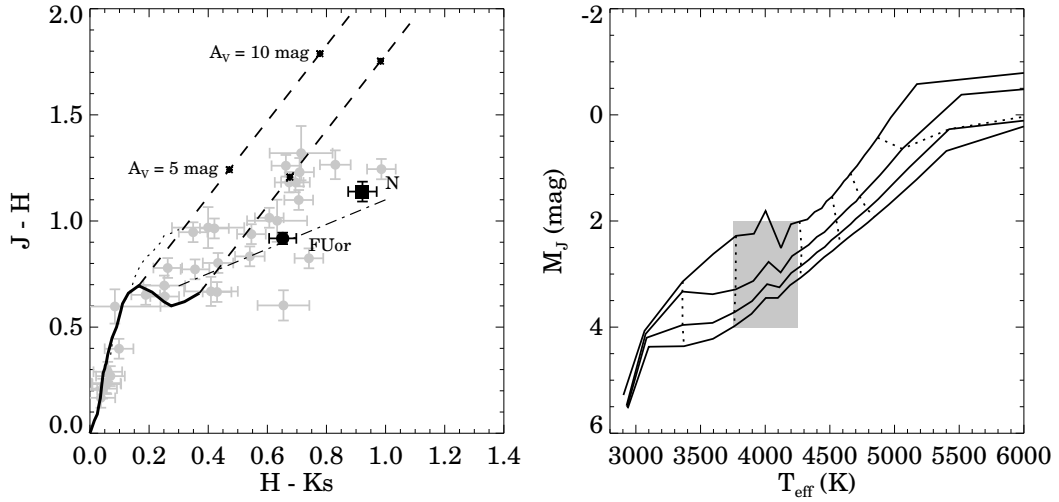


Fig. 2.— Left: Near-infrared color-color diagram. The main-sequence is marked by a solid line, the giant branch with dotted line (Koornneef 1983), the reddening path with dashed lines (Cardelli et al. 1989), and the T Tauri locus with dash-dotted line (Meyer et al. 1997). The black dot marks the FUor (2MASS J06593158–0405277), while the black square marks the N component (2MASS J06593168–0405224). Right: PMS evolutionary tracks for 0.5, 1.0, 1.5, and 2.0 Myr (from top to bottom) from Siess et al. (2000). The dotted lines mark stellar masses of 0.3, 0.5, 1.0, 1.5, 2.0, and 3.0 M_{\odot} (from left to right). The temperature range allowed by assuming that the central star is a late K or early M-type star with negligible reddening and the corresponding range in absolute J magnitudes is marked with a gray rectangle.

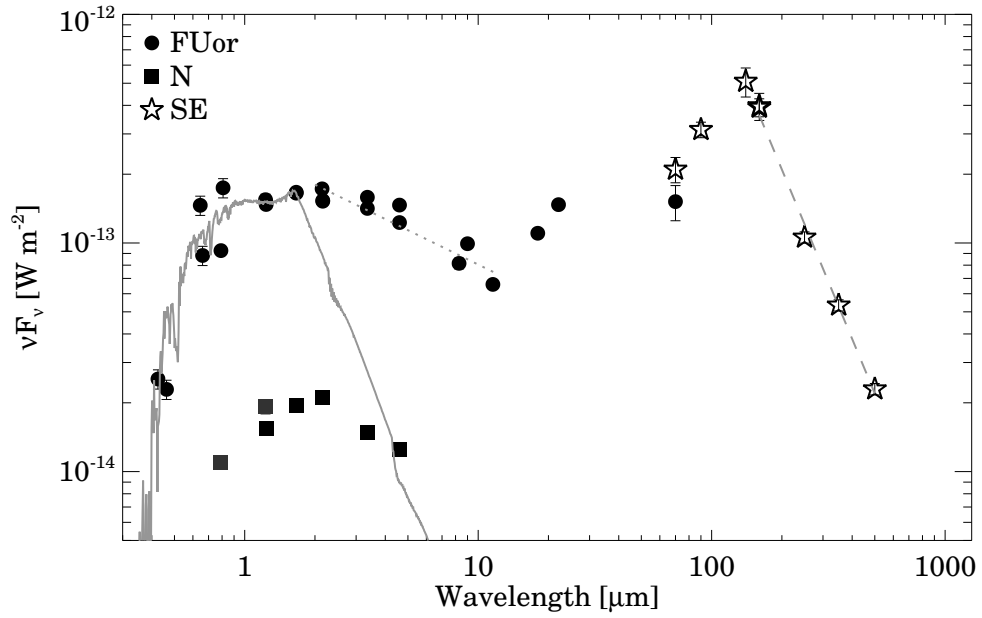


Fig. 3.— Pre-outburst SED of the FUor (2MASS J06593158–0405277) with black dots, the northern component (2MASS J06593168–0405224), and the SE (submillimeter) component. See Table 1 for the source of the data points. The gray curve is a 4000 K Kurucz model, the dotted line is a power law with a slope of -0.5 , and the dashed line is a power law with a slope of -2.5 .